*J. Fluid Mech.* (1973), *vol.* 57, *part* 2, *pp.* 321–336
*Printed in Great Britain*



# An inviscid model of two-dimensional vortex shedding

By R. R. CLEMENTS
Engineering Department, Cambridge University

(Received 22 June 1972)

An inviscid model of two-dimensional vortex shedding behind a square-based section is developed. The model uses a discrete-vortex approximation for the free shear layers. The motion of the shear layers is computed from the velocities of the discrete vortices, which in turn are derived through a Schwartz–Christoffel transformation of the section. The flow round the body is impulsively started from rest and initially develops symmetrically. The introduction of a small asymmetric disturbance results in asymmetric interaction of the shear layers amplifying into steady vortex-shedding motion.

The model is shown to predict the form of vortex shedding, the Strouhal number and some other flow quantities to a good degree of agreement with experimental results.

## 1. Introduction

In this paper a two-dimensional inviscid flow model is proposed for representing the flow in the near wake of a bluff-based body. The model uses an approximate representation of continuous vortex sheets in inviscid flow that has been used in the past by a number of workers for a variety of problems. The first use of the method was by Rosenhead (1931), who investigated a model of an infinite perturbed two-dimensional vortex sheet in which the sheet was represented by an array of line vortices with their axes in the direction of the vorticity of the sheet. Numerical analysis of this model then enabled Rosenhead to predict the rolling-up behaviour of the vortex sheet. Later improvements and additions to his work were made by Hama & Burke (1960) and Birkhoff & Fisher (1959).

The same fundamental approximation for the vortex sheets was used in a model of a pair of infinite parallel vortex layers described by Abernathy & Kronauer (1962). In their paper the four fundamental modes of perturbation of parallel vortex layers of opposite sign were obtained and the time development of one of these, the antisymmetric growing mode, then calculated numerically. The development and interaction of the two vortex layers was seen to give rise to the familiar von Kármán vortex street arrangement of localized concentrations of vorticity of opposite sign.

The same approximation was again used by Gerrard (1967), Sarpkaya (1968) and Laird (1971), who all describe models of flow behind circular cylinders in which the separated shear layers are approximated by the arrays of line vortices. Sarpkaya's method was to start the flow around the cylinder impulsively from rest and calculate the initial symmetric development. His work was later

extended by Davis (1970) to include the case of the asymmetric flow following some asymmetric disturbance of the original flow. Gerrard and Laird, however, chose to start their calculations from arbitrary flows which already included some vorticity in the flow field and calculate the subsequent periodic behaviour of these flows. Gerrard, Davis and Laird all found that periodic vortex shedding of the von Kármán pattern resulted in their calculations.

The flow around a circular cylinder is an attractive one to deal with theoretically since the boundary conditions on the cylinder can be easily satisfied by a simple image system. However, the points of separation of the shear layers from the cylinder are not fixed and this forced Gerrard, Sarpkaya, Laird and Davis to make various assumptions about the separation points in their calculations of the flow. The model described here is of the flow around a body with fixed separation points, this shape being chosen to obviate the need for any assumptions to be made about the separation position.

Other workers, notably Fromm & Harlow (1963), Thoman & Szewczyk (1969), Dawson & Marcus (1970) and Jordan & Fromm (1972), have approached the problem of periodic flow behind a bluff body by solving finite-difference analogues of the full Navier–Stokes equations in two dimensions. All of these works have an upper bound on the Reynolds number since the methods suffer from instability or require difference meshes of impracticably small size to obtain stability at high Reynolds numbers. In addition the solution of the complete equations is extremely costly in computer time.

## 2. Mathematical description of the model

The model proposed here is of the flow behind a bluff plane-based two-dimensional body having right-angle corners between the sides and rear face. The flow is assumed to remain attached on the side faces and to separate at the corners.

The model approximates the shear layers shed from the separation points of the body by arrays of line vortices. The motion of the shear layers in time is then represented by the evolution of the arrays of line vortices. The velocity of any vortex is the sum of the two-dimensional irrotational potential flow around the body and the velocity induced at the vortex position by all the other vortices. These velocities can be obtained by assuming the body to extend to infinity upstream (see figure 1) and then using a Schwartz–Christoffel transformation to project the exterior region of the body into an upper half plane with the boundary of the body along the real axis.

The transformation from the physical ($z$) plane to the transformed ($\lambda$) plane which transforms the rear corners of the body, $z = \pm is$, into the points $\lambda = \pm 1$ is given by

$$\left.\begin{aligned} z &= -(2is/\pi)\,[\sin^{-1}(\lambda) + \lambda(1-\lambda^2)^{\frac{1}{2}}], \\ \text{or} \quad z &= (2is/\pi)\,\{i\log[i\lambda + (1-\lambda^2)^{\frac{1}{2}}] - \lambda(1-\lambda^2)^{\frac{1}{2}}\}. \end{aligned}\right\} \tag{1}$$

From the complex-variable theory it is known that the complex potential $w = \phi + i\psi$, where $\nabla\phi = \mathbf{u}$, the velocity, and $\psi$ is the stream function, is a trans-

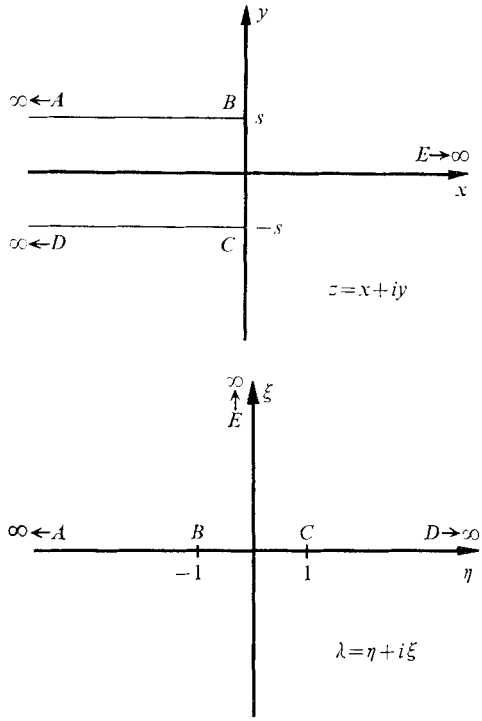


FIGURE 1. General arrangement of axes.

formal invariant. Also the flow field due to a vortex transforms into that due to a vortex of equal strength at the transform of the vortex position. Hence the velocity at any point of the fluid in the physical plane may be obtained by transforming the positions of all the vortices into the $\lambda$ plane, calculating the velocity at the transform of the required point and then returning this velocity to the physical plane through the relationship

$$u(z)-iv(z)=\frac{dw}{dz}=\frac{dw}{d\lambda}\frac{d\lambda}{dz}.$$

If the point whose velocity is required is also a vortex position the return to the $z$ plane is complicated by Routh's rule thus.

As the potential is a transformal invariant

$$w_{z_1}(z)-\frac{ik}{2\pi}\log(z-z_1)=w_{\lambda_1}(\lambda)-\frac{ik}{2\pi}\log(\lambda-\lambda_1),$$

where $w_{z_1}$ and $w_{\lambda_1}$ are the potentials at $z_1$ and $\lambda_1$ due to all causes except the vortex of strength $k$ at $z_1$, then

$$w_{z_1}(z)=w_{\lambda_1}(\lambda)-\frac{ik}{2\pi}\log\left(\frac{\lambda-\lambda_1}{z-z_1}\right).$$

Now if

$$\lambda=f(z)=f(z_1)+(z-z_1)f'(z_1)+\tfrac{1}{2}(z-z_1)^2f''(z_1)+O(z-z_1)^3,$$
$$\lambda-\lambda_1=(z-z_1)f'(z_1)+\tfrac{1}{2}(z-z_1)^2f''(z_1)+O(z-z_1)^3,$$

then $$w_{z_1}(z) = w_{\lambda_1}(\lambda) - \frac{ik}{2\pi}\log\left[f'(z_1) + \tfrac{1}{2}(z-z_1)f''(z_1) + O(z-z_1)^2\right],$$

$$\frac{dw_{z_1}}{dz} = \frac{dw_{\lambda_1}}{d\lambda}\frac{d\lambda}{dz} - \frac{ik}{2\pi}\left[\frac{\tfrac{1}{2}f''(z_1) + O(z-z_1)}{f'(z_1) + O(z-z_1)}\right]$$

$$= \frac{dw_{\lambda_1}}{d\lambda}\frac{d\lambda}{dz} - \frac{ik}{2\pi}\left[\tfrac{1}{2}f''(z_1) + O(z-z_1)\right]\frac{1}{f'(z_1)}\left[1 + O(z-z_1)\right].$$

Then as $z \to z_1$ and $\lambda \to \lambda_1$

$$\left.\frac{dw_{z_1}}{dz}\right|_{z_1} = \left.\frac{dw_{\lambda_1}}{d\lambda}\right|_{\lambda_1}\left.\frac{d\lambda}{dz}\right|_{z_1} - \frac{ik}{2\pi}\frac{f''(z_1)}{2f'(z_1)}.$$

The expression for $dw_{\lambda_1}/d\lambda$ is composed of the sum of the velocities induced at $\lambda_1$ by all the other vortices and the free-stream irrotational flow velocity. The irrotational flow used was composed of two components, the forms of both in each plane being illustrated in figure 2. In the physical ($z$) plane the first has a velocity $\mathbf{U} \to (U_0, 0)$ far up- and downstream and the second has a velocity $\mathbf{u} = (0, -pU_0)$ at $z = 0$ and $|\mathbf{u}| \to 0$ as $|z| \to \infty$. The second flow is a circulatory flow in the region of the base and was used to create the initial disturbance when the flow was started from rest (see § 3). Hence for most of the calculation $p = 0$. The expressions for $w(\lambda)$ are given in figure 2.

In order to maintain the boundary condition of zero flow across the body boundary it was necessary to prevent flow across $\xi = 0$ in the $\lambda$ plane. This was equivalent to having image vortices in $\xi < 0$ of opposite sign and equal strength to those in $\xi > 0$. Hence if at any time there are vortices of strengths $k_i$ at positions $z_1$ in the physical plane and $z_i = f(\lambda_i)$ the velocities $[dw/dz]_{z_i}$ are given by

$$\left.\frac{dw}{dz}\right|_{z_i} = \left[\sum_{\substack{j \\ j\neq i}} -\frac{ik_j}{2\pi}\frac{1}{\lambda_i - \lambda_j} + \sum_j \frac{ik_j}{2\pi}\frac{1}{\lambda_i - \bar{\lambda}_j} - \frac{4sU_0\lambda_i}{\pi} + \frac{4sp\mathbf{U}_0}{\pi}\right]\left.\frac{d\lambda}{dz}\right|_{z_i} - \frac{ik_i}{2\pi}\frac{f''(z_i)}{2f'(z_i)},$$

where $\bar{\lambda}$ denotes the complex conjugate of $\lambda$.

However, from (1),

$$dz/d\lambda = -(4is/\pi)(1-\lambda^2)^{\frac{1}{2}},$$

so

$$\frac{d\lambda}{dz} = f'(z) = \frac{i\pi}{4s}\frac{1}{(1-\lambda^2)^{\frac{1}{2}}},$$

$$f''(z)/2f'(z) = i\pi\lambda/8s(1-\lambda^2)^{\frac{3}{2}}$$

and

$$\left.\frac{dw}{dz}\right|_{z_i} = \left[\sum_{\substack{j \\ j\neq i}} -\frac{ik_j}{2\pi}\frac{1}{\lambda_i - \lambda_j} + \sum_j \frac{ik_j}{2\pi}\frac{1}{\lambda_i - \bar{\lambda}_j} - \frac{4sU_0\lambda_i}{\pi} + \frac{4spU_0}{\pi}\right]\frac{i\pi}{4s(1-\lambda_i^2)^{\frac{1}{2}}}$$

$$- \frac{ik_i}{2\pi}\frac{i\pi\lambda_i}{8s(1-\lambda_i^2)^{\frac{3}{2}}}. \tag{2}$$

Non-dimensionalizing with respect to $s$ and $U_0$ so that

$$k_j' = \frac{k_j}{U_0 s}, \quad z' = \frac{z}{s}, \quad u' = \frac{u}{U_0}, \quad v' = \frac{v}{U_0}, \quad w' = \frac{w}{sU_0}$$

gives

$$u_i' - iv_i' = \left.\frac{dw'}{dz'}\right|_{z_i'} = -\frac{1}{(1-\lambda_i^2)^{\frac{1}{2}}}\left[i\lambda_i - ip - \frac{k_i'\lambda_i}{16(1-\lambda_i^2)} + \sum_j \frac{k_j'}{8}\frac{1}{\lambda_i - \bar{\lambda}_j} - \sum_{\substack{j \\ j\neq i}} \frac{k_j'}{8}\frac{1}{\lambda_i - \lambda_j}\right]. \tag{3}$$

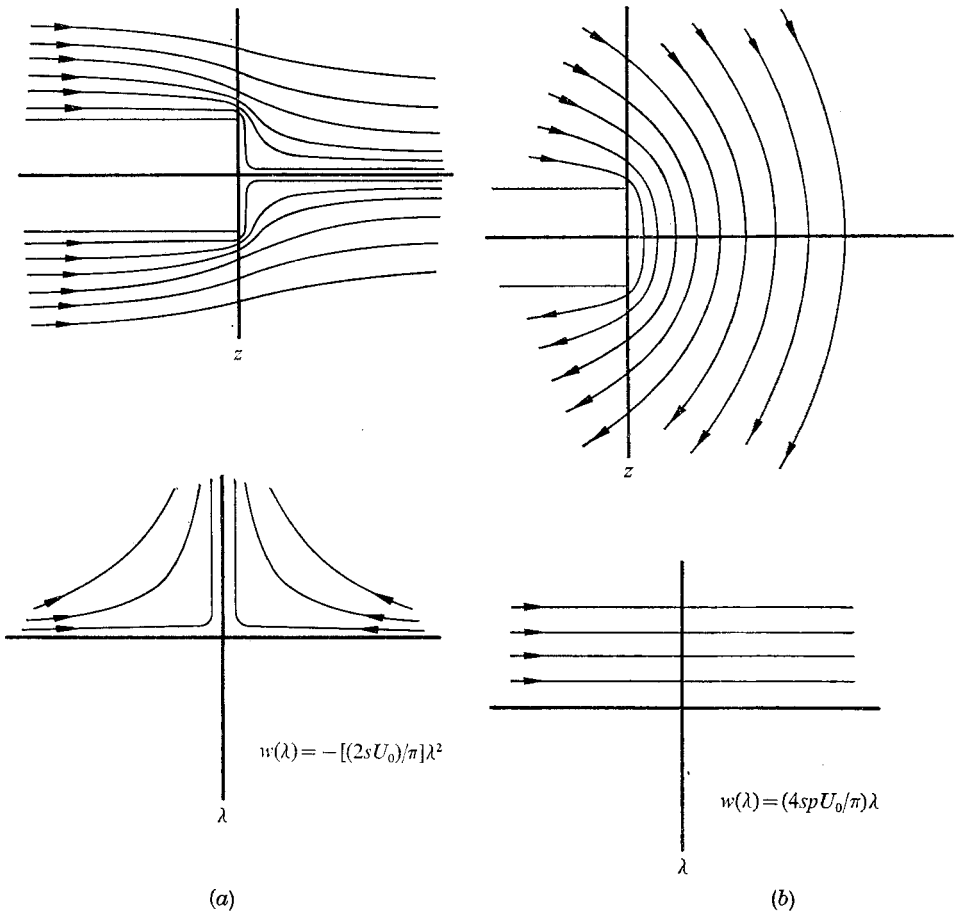


FIGURE 2. (*a*) First and (*b*) second irrotational inviscid flow and equivalent flow in transformed plane.

Hence the vortex velocities can be calculated for any given arrangement of line vortices in the physical plane. Two schemes for calculating the time development of the system were used:

$$\left.\begin{aligned} x'(t+\delta t) &= x'(t)+u'(t)\,\delta t,\\ y'(t+\delta t) &= y'(t)+v'(t)\,\delta t; \end{aligned}\right\} \tag{4a}$$

$$\left.\begin{aligned} x'(t+\delta t) &= x'(t)+\tfrac{1}{2}(3u'(t)-u'(t-\delta t))\,\delta t,\\ y'(t+\delta t) &= y'(t)+\tfrac{1}{2}(3v'(t)-v'(t-\delta t))\,\delta t. \end{aligned}\right\} \tag{4b}$$

The first has an error in any time step $O(\delta t^2)$ and the second an error $O(\delta t^3)$. The calculations performed with each scheme are described below.

The computations described in this paper were all carried out with the flow started impulsively from rest with no vorticity in the fluid. Vorticity, in the form of line vortices, was then introduced into the fluid from the two separation points. At an early stage some form of asymmetry was introduced into the flow field for a short time and the flow then allowed to develop. The separation points ($z = \pm is$) are singularities of the transformation, the effect being, as seen in (3),

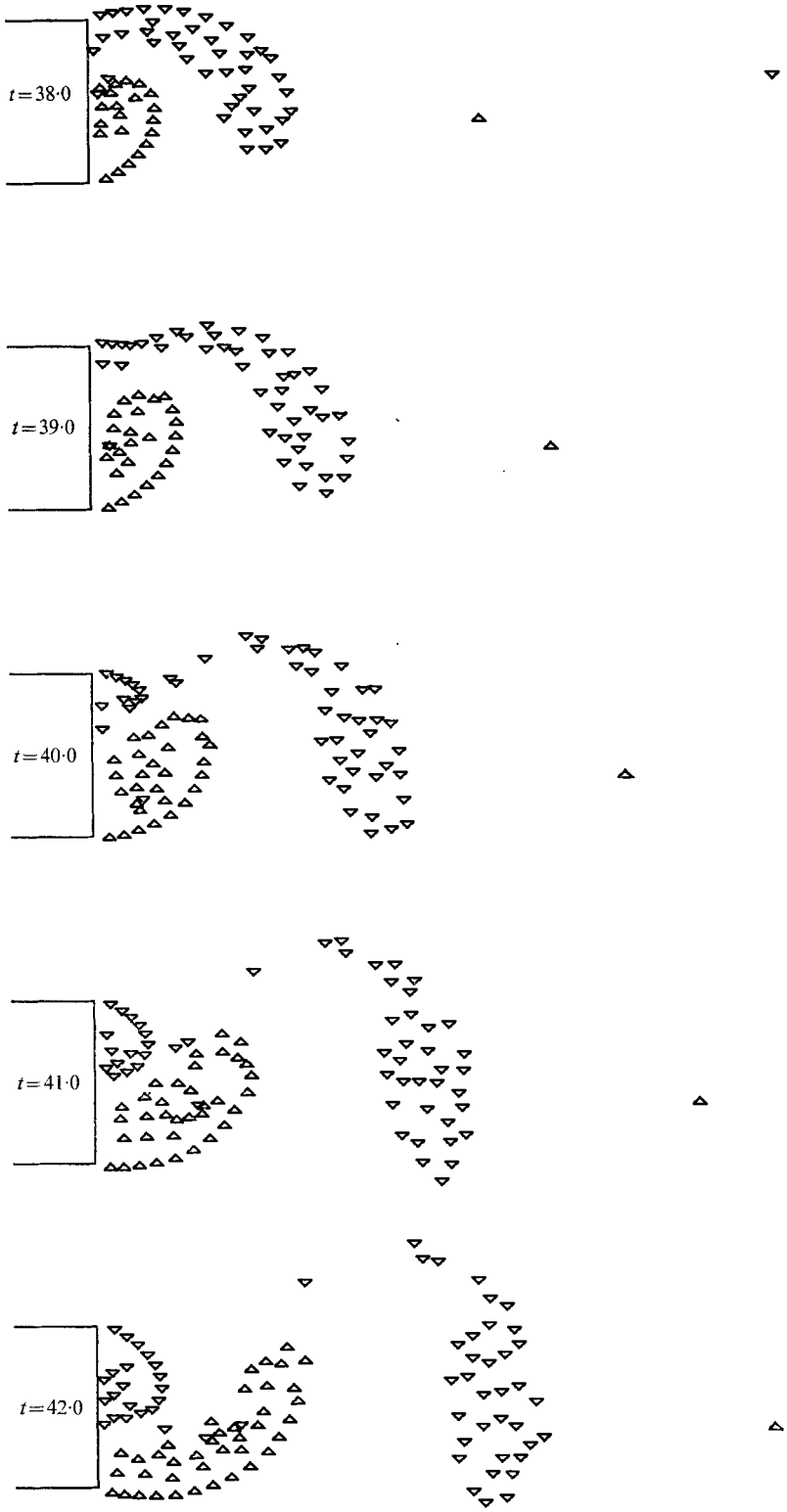


FIGURE 3. For legend see facing page.

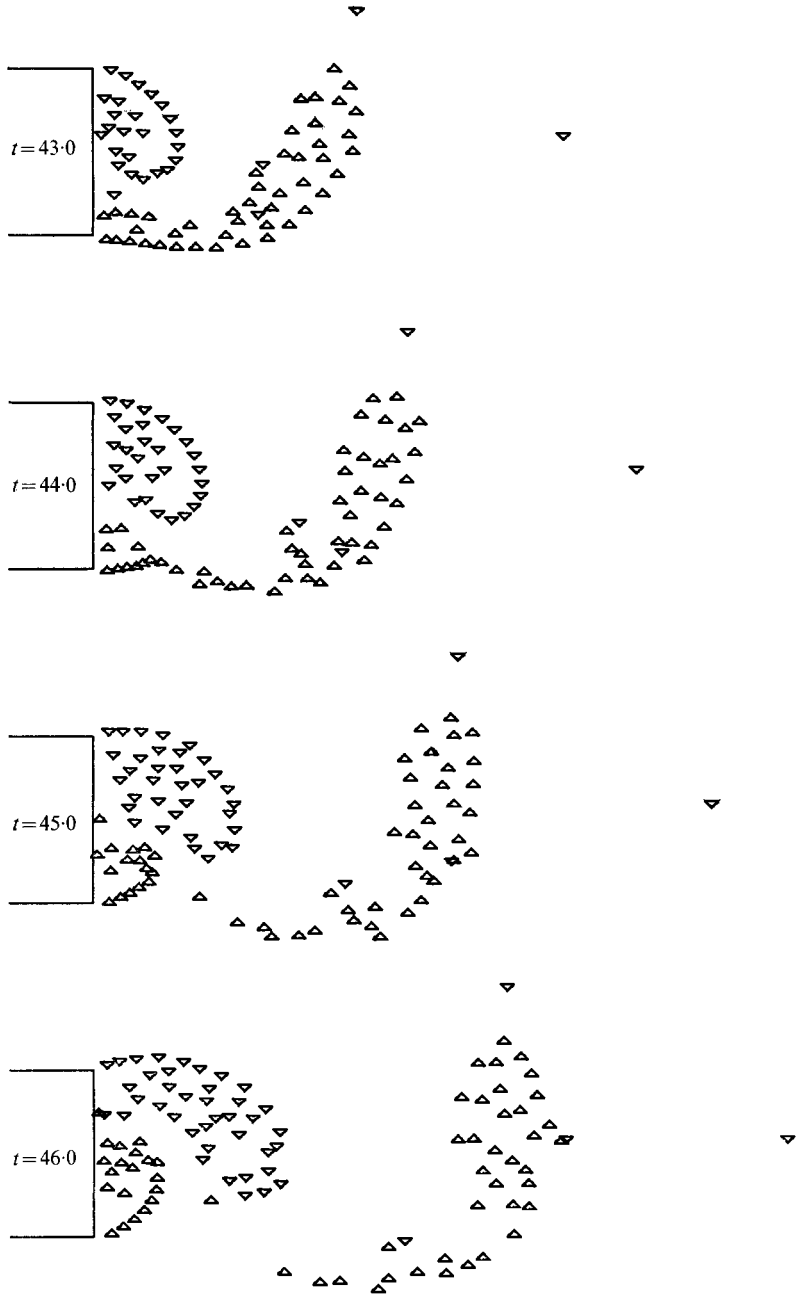


FIGURE 3. Vortex arrangements over one full cycle of steadily periodic flow. △, positive vortices; ▽, negative vortices.

to cause infinite velocities at these points through the factor $(1-\lambda^2)^{-\frac{1}{2}}$. However, another consideration also enters here. Were the fluid viscous, the velocity at the separation points would be zero to satisfy the no-slip condition, so the velocity with which the shear layer and hence the vortex in the model leaves the separation point is determined by the velocity $U_s'$ at the outer edge of the boundary layer. This velocity also determines the rate of vorticity shedding into the shear layers through the relationship $d\Gamma'/dt = \frac{1}{2}U_s'^2$. No attempt has been made to obtain any relationship between the 'boundary-layer thickness' used in the model and any physical flow parameter, instead a parameter $Y_I$ has been used such that, at its departure from the separation point, a newly created vortex moves with the velocity of the fluid at the point $z' = \pm(1+Y_I)i$ and has a strength $k'$ equal to $\Sigma \frac{1}{2}U_s'^2 \delta t$, where $U_s'$ is the velocity at the point $z' = \pm(1+Y_I)i$, $\delta t$ is the time step used in the calculation and the sum is over all the time steps since the last elementary vortex was introduced. The effect of varying the parameter $Y_I$ was then studied. Vortices were shed at intervals equal to various integral numbers of time steps, the interval remaining constant in any one calculation.

The vortices themselves were introduced from the actual separation points $z' = \pm i$. In some early calculations they were introduced into the flow at $z' = \pm(1+\frac{1}{2}Y_I)i$ but it was found that this resulted in a 'leakage' of fluid into the base region through the gap between the vortex rows representing the shear layers and the body sides. The mass flow involved could be considerable as the singularities at the corners caused large velocities in the gap.

Attempts were also made in early calculations to use the Kutta condition to determine the strength of newly introduced vortices but this gave rise to shear layers that separated at physically unrealistic angles to the free-stream direction and the attempts were not pursued.

Two further features of the model should be mentioned. First, in the absence of viscosity and a no-slip condition on the body boundary, it was found that individual line vortices could approach too close to the rear face of the body and this caused them to have unduly high velocities along the body (owing to the presence of the images in the lower half $\lambda$ plane). This was avoided by removing from the calculation vortices that approached closer than $0{\cdot}05s$ to the rear face. Physically this is equivalent to the destruction of vorticity in the shear layer by interaction with the boundary layer in that part of the cycle when the shear approaches very closely to the rear face.

Second, in order to keep the computation time within reasonable bounds, it was necessary to restrict the total number of line vortices to be handled by massing the effects of clusters of vortices into an equivalent single vortex whose strength was the sum of the individual strengths and placed at the centre of vorticity of the cluster. This process was invoked on clusters of elementary vortices that had formed close behind the body and passed off downstream beyond about $x/s = 4$. For examples of the sort of systems so treated see frames 5 and 9 of figure 3. The effect of this replacement is discussed below. These single equivalent vortices were retained in the flow throughout the subsequent calculation although their effect on the flow in the base region diminishes as they get further downstream.

## 3. Calculations

All the calculations described in this paper were programmed in Fortran and carried out on the Cambridge University Computer Laboratory's Titan (Atlas II) computer. Because of limitations on computing time available the computations were performed in blocks of 5 min duration and the results stored on magnetic disk file in between such blocks in a form that the programs could recover and use to continue the calculations. These periodic arrests were also used as an opportunity to carry out the replacement of large vortex clusters by their equivalent single vortex as mentioned above.

A large number of preliminary calculations were carried out to determine the optimum values of the parameter $\delta t$ and the interval between the introduction of successive elementary vortices. It was advantageous to make the latter fairly large as the time required to compute any set of velocities increases as the second power of the number of vortices involved. However, making the interval too large results in vortices of relatively large strength and wide spacing – a very crude approximation to the free shear layer. Similarly a large time step shortens the computation time but in this case the time step is limited by consideration of the ability of the vortices to follow the streamlines of the flow. Figure 4 illustrates this. The solid lines are 'true' streamlines of some steady curved flow. The broken line illustrates the path of a particle that proceeds with a constant velocity $U'(t)$ for a time $\delta t$, then with another velocity $U'(t+\delta t)$ for another $\delta t$ and so on. It can be seen that the effect will be to follow a path of smaller curvature than the 'true' path. In the model described here such a region exists in the corner formed by the back of the body and the free shear layer immediately after separation. If too large a time step $\delta t$ was used the elementary vortices were not able to follow the high curvature of the streamlines but broke through the line of vortices representing the emergent shear layer.

From these considerations the preliminary calculations indicated that a value of $\delta t = 0{\cdot}1$ with two time steps between the introduction of successive vortices would produce satisfactory results with the first-order time scheme (equation $(4a)$) and that $\delta t = 0{\cdot}16$ with two time steps between vortices would produce equivalent or better accuracy with the second-order scheme described (equation $(4b)$). The step lengths are given in terms of non-dimensional time $t$, which is related to real time $T$ by $t = U_0 T/s$. The second-order scheme was introduced during the work in order both to increase the accuracy and to reduce the computation time involved in the calculations. Since the work reported here was completed the programs have been modified to run on the University IBM 370/165 computer. Computation times for a typical calculation are 2 h for the first-order scheme and 30 min for the second-order method on Titan and 1·5 min for the second-order method on the IBM machine.

Many preliminary runs were also made to determine the importance of the size and type of the initial perturbation made to the symmetric flow. Amongst those tried were (i) a 20 % increase of strength of three successive vortices in one shear layer; (ii) a movement of $0{\cdot}2s$ of three or four successive vortices in one shear layer either up, down or downstream; (iii) a circulatory motion. These were

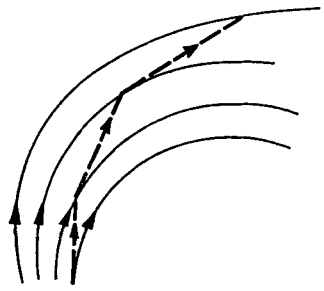

FIGURE 4. Illustration of numerical error in vortex paths in curved streamlines.

| Computation | $\delta t$ | $Y_I$ | Interval between introduction of vortices | Numerical scheme for time integration |
|---|---|---|---|---|
| $A$ | 0·1 | 0·1 | $2\delta t$ | (4$a$) |
| $B$ | 0·1 | 0·2 | $2\delta t$ | (4$a$) |
| $C$ | 0·1$\hat{6}$ | 0·1 | $2\delta t$ | (4$b$) |
| $D$ | 0·1$\hat{6}$ | 0·4 | $2\delta t$ | (4$b$) |

TABLE 1

relatively small perturbations compared with the whole flow field. It was found that if the perturbations were introduced at times of the order of $t = 2{\cdot}0$ or more the subsequent development tended to be fairly symmetric and amplification of the disturbance was too slow to be computationally feasible. If the disturbance was introduced earlier at around $t = 1{\cdot}0$, when there were relatively few vortices in the flow, then since most of these would be affected by the disturbance the amplification was much faster. Similarly, it was found that the fastest amplification resulted from a downstream disturbance of one of the shear layers and that disturbances in the positive or negative $y$ direction tended after a time to return to the original line of the shear layer but with a downstream perturbation present. All these are somewhat qualitative results but the indications were that the actual form of the initial disturbance had little bearing on the form of the subsequent development but affected the time needed for the disturbance to build up.

From these preliminary investigations emerged the circulatory disturbance used on three out of four of the final computations that were made. This disturbance consisted of the second form of steady irrotational flow mentioned in the previous section with the size of the factor $p$ determined by

$$p = \begin{cases} 0{\cdot}1 \sin(\frac{1}{3}\pi t) & (t < 3), \\ 0 & (t \geqslant 3). \end{cases}$$

When these preliminary investigations were complete four major computations were performed. For brevity these will be referred to as $A$, $B$, $C$ and $D$ and the characteristics of each are given in table 1.

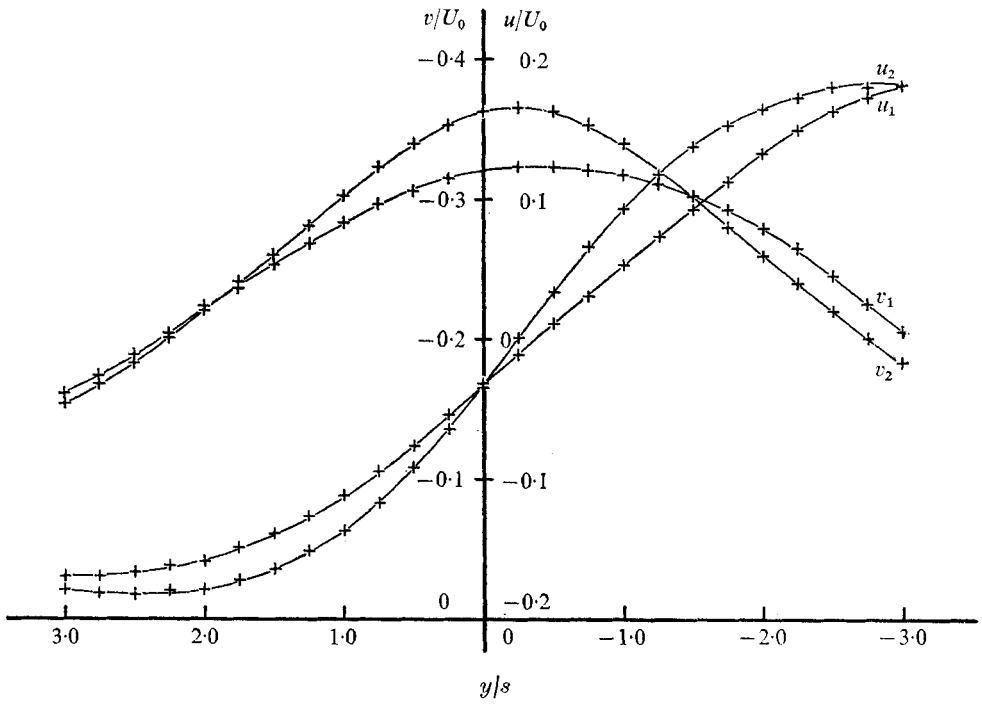


FIGURE 5. Comparison of $u$ and $v$ velocity components at $x/s = 3{\cdot}0$ due to shed vortex cluster $(u_1, v_1)$ and equivalent single vortex $(u_2, v_2)$ at $x/s = 5{\cdot}17$.

For computation $A$ the initial disturbance used was a downstream displacement of $0{\cdot}2s$ of three vortices of the lower shear layer at $t = 1{\cdot}0$, and for $B$, $C$ and $D$ the circulatory disturbance defined above was used.

A separate study was made of the effects of replacing the clusters of elementary vortices that separated from the near-wake flow (as in figure 3) by their equivalent single vortex. Calculations were made of the $x$ and $y$ components of the velocity due to the cluster and that due to the equivalent single vortex at points along a line $x =$ constant at a distance $2s$ upstream of the position of the single vortex and the two quantities compared. It can be seen from figure 3 that $2s$ is a typical separation between the centre of such a cluster and the rest of the elementary vortices at the time of replacement. The difference between the two sets of velocities induced at the points on the line $x =$ constant would decrease as the vortex cluster moved downstream. The results of a typical calculation are shown in figure 5. As a second approach to this aspect of the problem, a comparative run was made in which the results of replacing a cluster and not doing so were compared at a time $t = 1{\cdot}5$ later. The effect on the remaining vortices in the field near to the body was negligible.

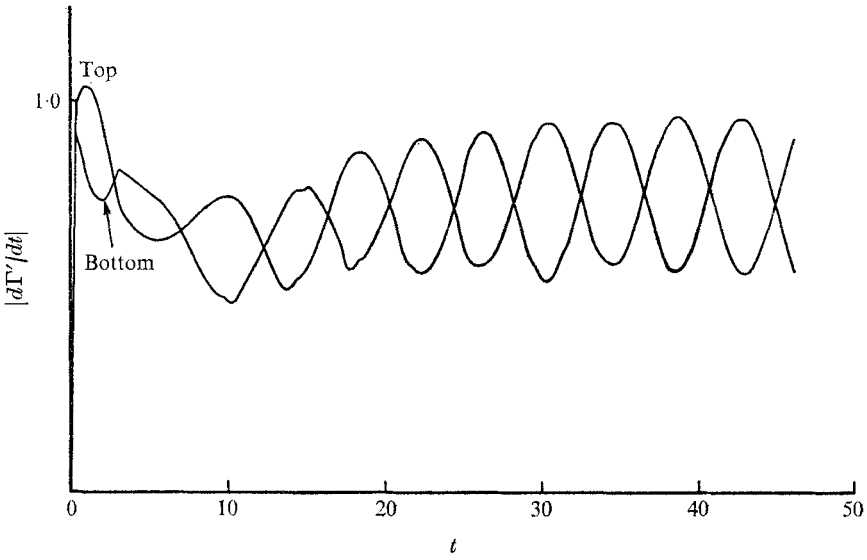


FIGURE 7. Rate of shedding of vorticity into shear layers from top and bottom separation points.

## 4. Results and comparison with experiment

The development of the flow after the impulsive start was similar in all of the calculations performed. There was an initial period after the perturbation was applied during which the asymmetry in the flow was amplified, leading to a final quasi-steady periodic flow in which vortex shedding occurred. The length of this initial period varied considerably with the size and type of initial disturbance. No systematic investigation of the exact relationship has been undertaken; rather, two quickly amplifying cases have been treated and the eventual periodic flow studied. In all of the major computations mentioned in the previous section the initial disturbance was steadily amplified by the flow with shedding of small vortices of increasing strength until the steadily periodic flow was attained, and this flow was then followed in the computations for two to four full cycles. Figure 3 shows the elementary vortex configurations for the final full cycle of computation *B*. Replacement of a shed system of elementary vortices by their equivalent single vortex, as described above, takes place just before frame 1 and between frames 5 and 6.

Figure 6 (plate 1) shows some schlieren photographs of the vortex shedding behind a blunt-based section of chord/base height ratio 20·0 obtained by Archibald (1971, private communication) by injection of freon through holes in the rear face of the section. It can be seen that the agreement between the shapes of the shear layers predicted by the calculations and those seen in the experiment is extremely good.

Figure 7 shows the rate of shedding of vorticity into the two shear layers as a function of time for computation *B*. It can be seen that this rate varies periodically and in fact the distinction between that part of the shear layer that feeds

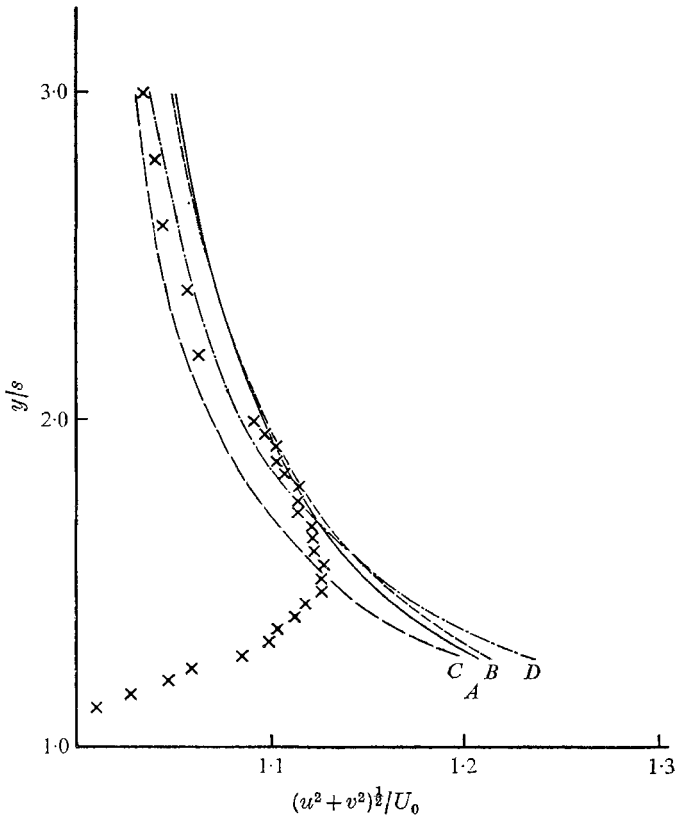


FIGURE 8. Mean velocity components on $x/s = 0$. ×, experimental points. Curves $A$, $B$, $C$ and $D$ are computational results.

into one vortex and that part which rolls back into the next vortex from the same side occurs at a minimum of vorticity strength in the shear layer. Frames 2 and 7 of figure 3 show the distinction occurring in the top and bottom shear layers respectively. The graph of figure 7 and similar graphs for the other computations were used to determine the Strouhal number of the shedding in each case. The Strouhal numbers were taken as the inverse of the average period of the last two full cycles of shedding and were non-dimensionalized with respect to the base height $2s$ and the free-stream velocity $U_0$. The results for computations $A$, $B$, $C$ and $D$ were 0·240, 0·240, 0·234 and 0·246 respectively, which agree well with the value 0·24 obtained by Bearman (1965) for the Strouhal number of shedding behind a bluff-based section of chord/base height ratio 6·0 at Reynolds numbers of $1{\cdot}4 \times 10^5$ and $2{\cdot}45 \times 10^5$.

When the final steadily periodic flow had been reached in all the major computations, values were obtained of the total velocity at various points in the flow field for comparison with experimental observations. For positions sufficiently removed from the shear layers the effect of the fundamental approximation of the model, the replacement of the shear layers by arrays of elementary line vortices, should be negligible. Hence, although one could not hope to predict the

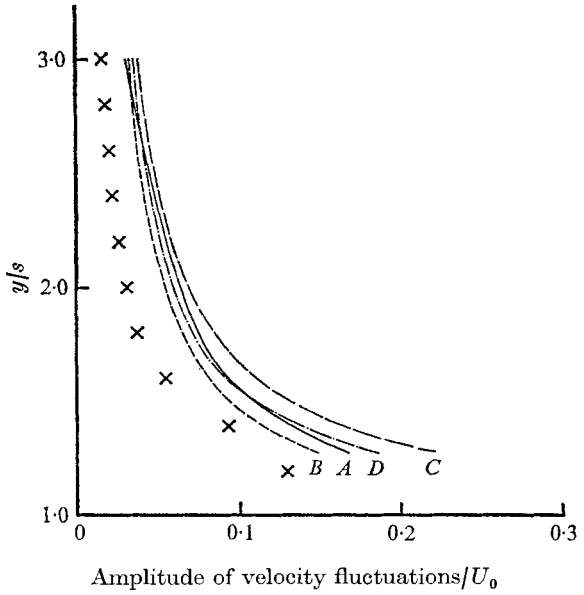


FIGURE 9. Amplitude of velocity fluctuation on $x/s = 0$. Notation as in figure 8.

signal that would be obtained from a hot wire anywhere within the wake, one would expect reasonable agreement at positions outside the wake. Values of the total velocity over the last full cycle at positions $z' = 1{\cdot}28i$, $1{\cdot}4i$, $1{\cdot}8i$, $2{\cdot}2i$, $2{\cdot}6i$, $3{\cdot}0i$ and $7{\cdot}0i$ were obtained for the four major computations. These seven sets of velocities were used for comparison with an experiment in which hot-wire measurements of the total velocity and the amplitude of velocity fluctuations were made at positions in the plane of the base of a blunt-based section of chord/base height ratio 6·0 at a Reynolds number of $2{\cdot}08 \times 10^4$. The hot wire was calibrated and then mean and r.m.s. measurements of the signal were made and the mean velocity and the amplitude of velocity fluctuations derived. These are compared with the results obtained from the calculations in figures 8 and 9. In both the calculations and the experiments the velocities were expressed as a fraction of the velocity at the point $z' = 7{\cdot}0i$ in order to maintain comparability. It can be seen that the model predicts the mean velocity extremely well for a distance $y/s$ greater than about 0·6 from the separation point. Nearer than this the effect of the boundary layer, which is not modelled in the computations, causes the calculated values to exceed the experimental ones. The agreement between the amplitudes of oscillation is not so good although the general shape and trend of the calculated curves agrees with the experimental results.

Another effect that is apparent in figure 3 is the shape of the clusters of elementary vortices as they move away from the immediate neighbourhood of the base of the body. At first sight they appear to be extremely elongated in the cross-wake direction. It must be borne in mind, however, that the elementary vortices of the clusters are not all of equal strength. The stream function due to one such cluster from computation $B$ taken in isolation has been calculated, and the streamlines, with elementary vortex positions shown for comparison, are

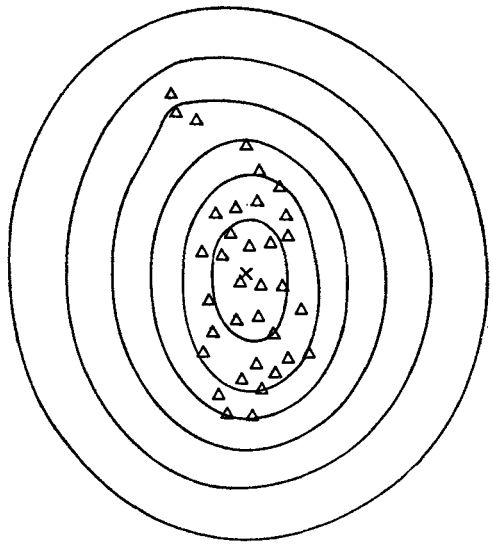

FIGURE 10. Streamlines due to shed vortex cluster in isolation. (The cross indicates the centre of vorticity of cluster.)

presented in figure 10. It can be seen that even such a wide spatial distribution of vorticity gives streamlines that have still not too greatly departed from the circular ones arising from an idealized concentrated point vortex. Similar calculations performed on several systems of elementary vortices taken from the other computations confirm this finding.

A number of workers have, in the past, investigated the relationship between the amount of vorticity generated in each shear layer before separation and the amount that finally appears in the fully formed street vortices further downstream for various bluff bodies. Fage & Johansen (1927) found the latter to be between 51 % and 65 % of the former for a flat plate set at right angles to the free-stream flow. Wood (1964) investigated the same ratio for a truncated aerofoil of chord/base height ratio 3·6 with base bleed and found that it decreased from 50 % at zero bleed as the bleed rate increased. Nielsen (1969), in a later experiment, found that the percentage was 66 % for the same body with no base bleed. The computations described in this paper show amounts varying between 87 % and 94 % of the shed vorticity in the shear layers appearing in the rolled-up vortices. The loss of vorticity in the computations arises from two mechanisms: first, the destruction of vorticity at the rear face of the body mentioned in § 2, and second, a small amount of cancellation between elementary vortices of opposite sign which enter the same rolled-up vortex core. The discrepancy between the computations and the experiments mentioned can probably be accounted for by the fact that the computations are essentially inviscid and the mechanism whereby much of the vorticity is lost must be viscous in nature.

## 5. Conclusions

The model proposed in this paper has been shown to be capable of predicting the dominant features of the flow behind a bluff-based section. The form of the vortex shedding, the Strouhal number and some mean flow velocities near to but outside the wake are all predicted to a high degree of accuracy. The model is, however, inviscid and hence cannot be expected to predict flow situations which are governed by predominantly viscous mechanisms. The underlying principle of the model could provide a powerful tool for the prediction of flows in a large number of other similar situations at relatively little expense of computer time and could also enlarge understanding of bluff-body flows by making possible the isolation of viscous-dominated flow features from inviscid flow features.

The author would like to thank Dr D. J. Maull, who supervized this work, for his many helpful suggestions and enlightening discussions. The support of the S.R.C. in giving a maintenance award is acknowledged.

REFERENCES

ABERNATHY, F. H. & KRONAUER, R. E. 1962 The formation of vortex streets. *J. Fluid Mech.* **13**, 1.

ARCHIBALD, F. 1971 Private communication.

BEARMAN, P. W. 1965 Investigation of the flow behind a two-dimensional model with a blunt trailing edge and fitted with splitter plates. *J. Fluid Mech.* **21**, 241.

BIRKHOFF, G. D. & FISHER, J. 1959 Do vortex sheets roll up? *Rendi. Circ. Math. Palermo*, series 2, vol. 8, p. 77.

DAVIS, D. M. 1970 An analytic study of separated flow about a circular cylinder. M.Sc. thesis, Naval Postgraduate School, Monterey.

DAWSON, C. & MARCUS, M. 1970 DCM – a computer code to simulate viscous flow about arbitrarily shaped bodies. *Proc. Heat Trans. Fluid Mech. Inst.* p. 323.

FAGE, A. & JOHANSEN, F. C. 1927 On the flow of air behind an inclined flat plate of infinite span. *Proc. Roy. Soc.* A **116**, 170.

FROMM, J. E. & HARLOW, F. H. 1963 A numerical solution of the problem of vortex street development. *Phys. Fluids*, **6**, 1975.

GERRARD, J. H. 1967 Numerical computation of the magnitude and frequency of the lift on a circular cylinder. *Phil. Trans. Roy. Soc.* **261**, 137.

HAMA, F. R. & BURKE, E. R. 1960 On the rolling up of a vortex sheet. *University of Maryland Tech. Note*, BN-220.

JORDAN, S. K. & FROMM, J. E. 1972 Oscillatory drag, lift and torque on a circular cylinder in a uniform flow. *Phys. Fluids*, **15**, 371.

LAIRD, A. D. K. 1971 Eddy formation behind circular cylinders. *Proc. A.S.C.E., Hydraulics Div.* **97**, 763.

NIELSEN, K. TH. W. 1969 Vortex formation in a two dimensional periodic wake. Ph.D. thesis, Oxford University.

ROSENHEAD, L. 1931 The formation of vortices from a surface of discontinuity. *Proc. Roy. Soc.* A **134**, 170.

SARPKAYA, T. 1968 An analytic study of separated flow about circular cylinders. *A.S.M.E. J. Basic Engng*, **90**, 511.

THOMAN, D. C. & SZEWCZYK, A. A. 1969 Time dependent viscous flow over a cylinder. *Phys. Fluids*, **12** (suppl. II), II 76.

WOOD, C. J. 1964 The effect of base bleed on a periodic wake. *J. Roy. Aeron. Soc.* **68**, 477.

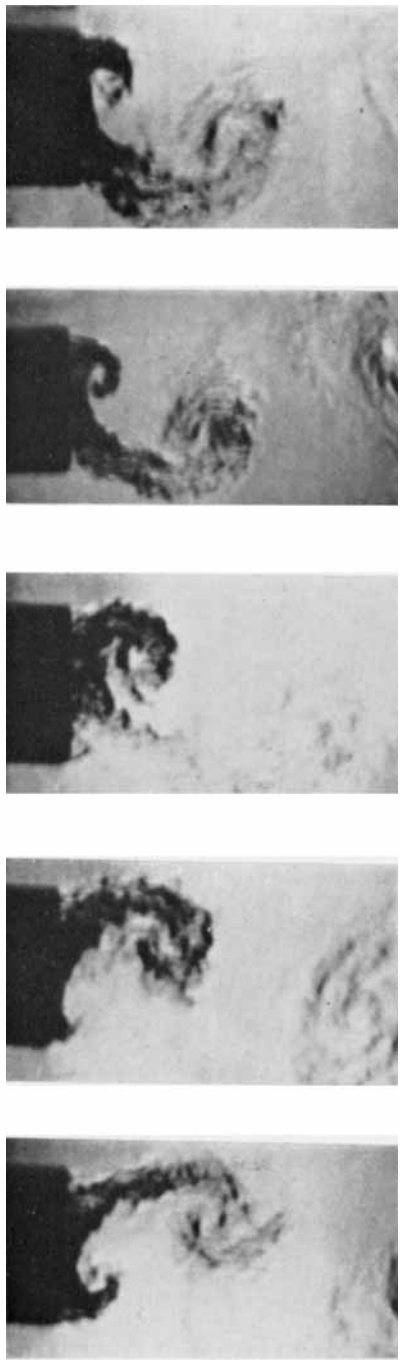

FIGURE 6. Schlieren photographs of vortex shedding from Archibald.